ATLAS NOTE

ATLAS-CONF-2012-107

August 11, 2012

A general search for new phenomena with the ATLAS detector in pp collisions at $\sqrt{s} = 7$ TeV

The ATLAS Collaboration

Abstract

This note presents a model-independent general search for new physics in proton proton collisions at a centre-of-mass energy of 7 TeV with the ATLAS detector at the LHC. The data set, recorded by the ATLAS experiment during 2011, corresponds to a total integrated luminosity of 4.7 fb^{-1}. Event topologies involving isolated electrons, photons, muons, jets, b-jets and missing transverse momentum are investigated. The events are subdivided according to their final states into 655 exclusive analysis channels. For each channel, a search algorithm tests the compatibility of the effective mass distribution in data against the distribution in the Monte Carlo simulated background. Although this search approach is less sensitive than optimized searches for specific models it provides a more comprehensive investigation for new physics signals. No significant deviations between data and the Standard Model expectations have been observed.

1   Introduction

It is well known that the Standard Model (SM) of particle physics cannot be a complete theory of fundamental interactions. It is instead likely to be a low energy manifestation (or an effective theory) of an underlying theory which would manifest itself at higher energies. There are many compelling reasons to believe that first signs of new physics may appear at LHC energies. In particular, new particles could be found, which might provide a solution for the cancelation of quadratic mass divergences that would accompany a SM Higgs boson or might point to the possibility that Dark Matter is made of new fundamental particles with a mass below the TeV scale. The LHC data have been used to search for various signals of new physics and stringent limits have been set on several models of Supersymmetry and other new phenomena. Although these searches cover already a wide variety of possible event topologies, they do not explore them all. Events caused by new interactions or new particles might still be hidden in the LHC data. The approach described in this note adresses this important issue with a model-independent search strategy. The search is designed to be comprehensive for new physics signals appearing at high transverse momenta rather than being optimized for specific channels or signals. The approach is not sensitive to final states with low transverse momentum or small signals in channels with large backgrounds.

Model-independent searches have been performed already at the D0 [1], H1 [2], CDF [3] and CMS [4] experiments. The strategy presented here is based on the approach taken by the H1 experiment. All event topologies involving electrons, photons, muons, jets, b-tagged jets and missing transverse momentum are investigated in a single analysis. The effective mass distribution of each final state is scanned for deviations from the Standard Model prediction. A statistical search algorithm looks for the region of largest deviation between data and the Standard Model prediction. The Standard Model prediction is constructed purely from Monte Carlo simulations. The approach identifies the largest deviations from the Monte Carlo implementation of the Standard Model prediction at ATLAS. If a significant deviation is found, a dedicated analysis will be required to determine if the deviation is caused by a mismodelling of the Standard Model prediction, a signal of new physics or other effects.

The note is organized as follows. Section 2 includes a description of the ATLAS detector. Section 3 describes the Monte Carlo prediction, section 4 the event selection and section 5 the systematic uncertainties. The statistical scanning algorithm and the results are presented in section 6.

2   The ATLAS experiment

ATLAS [5] is a multipurpose particle physics apparatus with a forward-backward symmetric cylindrical geometry and nearly 4π coverage in solid angle.[1] The layout of the detector is dominated by four superconducting magnet systems, which comprise a thin solenoid surrounding inner tracking detectors (ID) and three large toroids supporting a large muon tracker (MS). In the pseudorapidity region $|\eta| < 3.2$, high-granularity liquid-argon (LAr) electromagnetic (EM) sampling calorimeters surround the solenoid magnet. An iron-scintillator tile calorimeter provides hadronic coverage over $|\eta| < 1.7$. The end-cap and forward regions, spanning $1.5 < |\eta| < 4.9$, are instrumented with LAr calorimetry for both EM and hadronic measurements.

The data sample used in this analysis was recorded in 2011 at a centre-of-mass energy of 7 TeV with single muon, electron, jet, or combined jet and missing transverse momentum triggers. Application of beam, detector and data-quality requirements results in a data set with a total integrated luminosity of 4.7 ± 0.2 fb^{-1}[6].

---

[1] ATLAS uses a right-handed coordinate system with its origin at the nominal interaction point in the centre of the detector and the z-axis along the beam pipe. Cylindrical coordinates (r, ϕ) are used in the transverse plane, ϕ being the azimuthal angle around the beam pipe. The pseudorapidity η is defined in terms of the polar angle θ by $\eta = -\ln\tan(\theta/2)$.

3 Monte Carlo samples

In this search the Standard Model prediction is modelled by Monte Carlo (MC). In general good agreement is found between ATLAS data and Monte Carlo simulations. All dominant processes are considered for the Standard Model estimate: W+jets, Z+jets, top quark pair, multijet, prompt photon, diboson and single top production. Non-collision backgrounds were studied in several ATLAS analyses with identical object selection criteria and these backgrounds were found to give a negligible contribution [7].

Multijet production
Simulated multi-jet events are generated with PYTHIA [8] v6.4.21, which uses $2 \rightarrow 2$ leading order (LO) matrix elements (ME) with the MRSTMCal PDF set [9]. The large uncertainty in the cross section of multi-jet processes is discussed in section 5.2.

W+ jet and Z+ jet production
Electroweak gauge boson production in association with jets is generated using ALPGEN [10], which includes LO electroweak and QCD contributions for multipartons hard processes. Jet production is generated with up to six parton matrix elements and the samples are generated with the MLM matching scheme. The generator is interfaced to HERWIG [11] for showering and fragmentation and JIMMY [12] for the underlying event. All samples use the CTEQ6L1 [13] parton density. The obtained cross-sections are scaled to the next-to-next-to-leading order (NNLO) FEWZ [14] prediction. Contributions from Wbb, Wcc, Wc, and Zbb are included with separate ALPGEN samples. As ALPGEN does not match heavy flavour quark jets explicitly, the same final state is included in multiple samples. An overlap removal scheme is applied to avoid double counting of events. This is accomplished by a simple ΔR matching scheme. Additional scaling factors of 1.63 ± 0.76 and 1.11 ± 0.35 are applied to the Wbb/Wcc and the Wc samples respectively to account for the measured cross-section of W in association with b jets [15, 16].

γ+jets and γ pairs
Photon plus jets samples are generated with PYTHIA in a similar way to the multi-jet samples. Prompt diphoton samples are generated with PYTHIA in bins of $m_{\gamma\gamma}$. These samples include the hard matrix elements $gg \rightarrow \gamma\gamma$ and $q\bar{q} \rightarrow \gamma\gamma$. A filter is applied to select only events were the two photons have $p_T > 15$ GeV.

W/Z+γ
The $W\gamma$ samples are generated using ALPGEN in a similar way to the $W + jets$ samples. A generator level filter requiring at least one photon with $p_T > 10$ GeV is applied. The $Z\gamma$ process is generated with MadGraph [17] with parton showering and fragmentation simulated by PYTHIA. A generator level filter requiring at least one lepton with $p_T > 10$ GeV and $|\eta| < 2.5$ and one photon with $p_T > 7$ GeV and $|\eta| < 2.5$ is applied. The PDF set CTEQ6L1 is used for these samples. No scaling of the cross sections is applied. Madgraph is also used to generate $V + \gamma\gamma$ samples, with a leading-order matrix element. A K-factor of 2.0 ± 0.3 is chosen for $Z + \gamma\gamma$, based on Ref.[18]; and a K-factor of 3 ± 3 for $W\gamma\gamma$ based on the observed differences between the LO and next-to-leading order (NLO) calculations, as discussed in [19].

Top quark pair and single top production
The primary $t\bar{t}$ samples, with fully leptonic or semileptonic decays, are produced with ALPGEN, including up to 5 partons in the matrix element. Separate samples for $t\bar{t}b\bar{b}$ and $t\bar{t}c\bar{c}$ are used, after removing their overlap with the light flavour samples. Fully hadronic $t\bar{t}$ decays are simulated using MC@NLO [20, 21]. All samples are normalized to the NLO plus next-to-leading log (NLL) calculation [22]. Single top

events are generated using the MC@NLO program which includes full NLO corrections to the matrix element for the hard process. Final state parton showering and underlying event simulation is performed through interfaces to `HERWIG` and `JIMMY` respectively. A top quark mass of 172.5 GeV is assumed. The `CT10` PDF set [23] is used in both the single top and top quark pair samples for the matrix element, the parton shower, and the underlying event.

Top and vector boson production

Top quark pair production may also occur with an additional boson ($t\bar{t} + V$). These samples are generated using the `MadGraph`[17] LO generator with `PYTHIA` for showering. Cross sections are normalized to NLO [24, 25]. An additional sample, generated with `WHIZARD` [26] is used for $t\bar{t} + \gamma$ production. Both samples use the `CTEQ6L1` parton density functions.

Diboson production

WW, WZ and ZZ events are simulated using `HERWIG`, including off-shell boson contributions. A filter is applied to select events with at least one lepton with $p_T > 10$ GeV and $|\eta| < 2.8$ and the mass of the off-shell W or Z boson greater than 20 GeV. The `HERWIG` WW sample only describes opposite sign WW production. An additional sample, generated at tree-level with `MadGraph` is used for same sign production, and is not filtered at generator level. The `HERWIG` samples do not include in their computation diagrams with internal conversions and their interference.

Supersymmetric signal events

Benchmark signals were generated with `HERWIG++` [27] v2.4.2 in the CMSSM/MSUGRA model. These samples are normalised using NLO cross sections determined by `PROSPINO` [28] v2.1. For all non-`PYTHIA` samples `HERWIG++` or `HERWIG-6.510` [11] is used to simulate parton showering and fragmentation, while `JIMMY` [12] v4.31 is used to generate the underlying event. All samples are produced using an ATLAS 'tune' [29] and a full detector simulation [30].

4 Event Selection and classification

4.1 Object definition

Jet candidates are reconstructed using the anti-k_t jet clustering algorithm [31, 32] with a distance parameter of 0.4. The jet algorithm uses clusters of calorimeter cells seeded by those with energy significantly above the measured noise. Jet momenta are constructed by performing a four-vector sum over these cell clusters, treating each as an $(E, \vec{p})$ four-vector with zero mass. These jets are corrected for the effects of calorimeter non-compensation and inhomogeneities by using p_T- and η-dependent calibration factors based on MC corrections validated with extensive test-beam and collision-data studies [33]. Only jet candidates with $p_T > 20$ GeV and $|\eta| < 4.9$ are subsequently retained.

Jets arising from b-quarks are identified using information about track impact parameters and reconstructed secondary vertices [34]; the b-tagging algorithm is based on a neural network using the output weights of various b-tagging algorithms as input. A tight operating point at a b-tagging efficiency of 60% is used for which the algorithm provides a rejection factor of approximately 200-400 for light-quark and gluon jets and a rejection of approximately 7-10 for charm jets.

Electron candidates are required to have $p_T > 10$ GeV, to have $|\eta| < 2.47$, to pass the 'medium' electron shower shape and track selection criteria of Ref. [35], and to be outside problematic regions of the calorimeter. Muon candidates are reconstructed by combining tracks in the ID and MS. Muons are required to have $p_T > 10$ GeV and $|\eta| < 2.4$. Photon candidates are required to pass the tight identification

criteria [36]. Photons are required to lie in the fiducial region $|\eta| < 1.37$ or $1.52 < |\eta| < 2.37$ and to have a $p_T > 20$ GeV.

Following the steps above, overlaps between candidate jets with $|\eta| < 2.5$, leptons and photons are resolved using the method of Ref. [37] as follows. First, any such jet candidate lying within a distance $\Delta R = \sqrt{(\Delta\eta)^2 + (\Delta\phi)^2} < 0.2$ of an electron or photon is discarded. Then the whole event is rejected if any electron candidate remains in the calorimeter transition region $1.37 < |\eta| < 1.52$ between barrel and end-cap. Finally, any lepton or photon candidate remaining within a distance $\Delta R = 0.4$ of such a jet candidate is discarded.

The measurement of the missing transverse momentum two-vector $\vec{P}_T^{\text{miss}}$ (and its magnitude E_T^{miss}) is then based on the transverse momenta of all remaining jet and lepton candidates and all calorimeter clusters not associated to such objects. Thereafter, the remaining lepton and jet candidates are considered "reconstructed", and the term "candidate" is dropped. The same object identification and selection criteria are applied to data and Monte Carlo events.

4.2 Event selection

The ATLAS experiment records events in different physics streams depending on the sets of trigger criteria used. All events in the jet and missing transverse momentum (JetTauEtmiss) stream, the electron and photon (EGamma) stream and the Muon stream are considered for this analysis. The same event can be contained in more than one stream.

The detailed trigger specification varies throughout the stream and data-taking period. To remain at a high trigger efficiency events are only selected if they fulfill one of the cuts listed in Table 1. The trigger efficiency for events in the jet stream is above 98% for $E_T^{\text{miss}} > 160$ GeV and a reconstructed jet with $p_T > 130$ GeV [7]. In the electron stream, the electron trigger selects events containing one or more electron candidates, based on the presence of a cluster in the electromagnetic calorimeter, with a shower shape consistent with that of an electron. The transverse energy threshold at the trigger level ranges between 20-22 GeV, depending on the luminosity. The trigger efficiency is above 95% [38]. In the muon stream, the muon trigger selects events containing one or more muon candidates based on tracks identified in the MS and ID. The muon trigger p_T threshold is 18 GeV. The plateau efficiency ranges from about 70% in the barrel region to 88% in the endcaps.

Following the object reconstruction described above, events are discarded if they have any jets failing quality selection criteria designed to suppress detector noise and non-collision backgrounds [7], or if they lack a reconstructed primary vertex associated with five or more tracks.

4.3 Event classification

The events are subdivided, depending on the number and types of objects reconstructed in the event, into exclusive classes. Events with an isolated calorimetric object in the considered phase space which is not identified as a photon, electron or jet are discarded from the analysis in order to minimise wrong classifications. The subdivision can be regarded as a classification according to the most important features of the data. The lower p_T cuts and labels used for each object are summarized in Table 2. A lower cut on the p_T of the leading jet of 500 GeV is applied for the JetTauEtmiss stream if $E_T^{\text{miss}} < 130$ GeV, to reduce the analysis sensitivity to the limited number of multi-jet Monte Carlo events generated at low p_T.

5 Systematic uncertainties

The following sources of systematic uncertainties are taken into account.

Stream	trigger requirement
Muon	muon $p_T > 20$ GeV
EGamma	electron $p_T > 25$ GeV
JetTauEtmiss	jet $p_T > 130$ GeV & $E_T^{miss} > 160$ GeV or jet $p_T > 350$ GeV

Table 1: List of the p_T cuts used for each object in order to have a fully efficient trigger.

object	jet	b-jet	electron	muon	photon	E_T^{miss}
label	j	b	e	μ	γ	ν
lower p_T cut	50 GeV	50 GeV	25 GeV	20 GeV	40 GeV	130 GeV

Table 2: List of objects used for the event classification with their labels and lower p_T cuts. A lower cut on the leading jet of 500 GeV is applied for the JetTauEtmiss stream if $E_T^{miss} < 130$ GeV.

5.1 Experimental uncertainties

The uncertainty on the luminosity is 3.9% [6]. The jet energy scale uncertainty estimate is based on Monte Carlo studies and in-situ measurements and is provided in bins of $|\eta|$ and p_T. The scale is varied up and down within its uncertainty. The jet energy resolution uncertainty is also considered. It can impact the background predictions, mainly by changing the number of reconstructed jets in each event class. The b-tagging systematics considers the uncertainty on the b-tagging efficiency for b, c and light jets. MC events have been re-weighted to match the expected number of interactions per bunch crossing in data. A systematic uncertainty related to the pileup uncertainty is determined by comparing the nominal reweighting with a shift in the weight scale of 10%.

The experimental uncertainties and the uncertainty due to the limited number of MC events are in almost all channels the dominating uncertainties.

5.2 Theoretical uncertainties

All MC samples are normalized to their most accurate inclusive cross sections. Not using any data-driven technique to estimate the backgrounds, we rely purely on MC predictions. For the purpose of this general search, values have been chosen, which represent typical theoretical uncertainties of the models and generators used in the analysis. Those values are motivated by studies and results of dedicated searches and measurements by the ATLAS collaboration at high transverse momenta. As outlined in the introduction of this paper, any significant difference between data and SM Monte Carlo expectation will require a dedicated study of the backgrounds with control regions and data driven techniques. Such studies would be done a posteriori.

The following theoretical uncertainties are assigned per subprocess. Due to the tight requirements in the object selections, they are however of little importance for most of the event classes considered. The multi-jet production process is available only at leading-order, but higher jet multiplicities are quite well modelled with the parton shower approach. We assigned a systematic uncertainty of 30% in agreement with Ref. [39]. These uncertainties do not include fake lepton production which might play a role for some lepton channels. We assigned therefore an uncertainty of 100% for the multi-jet production contribution in channels with leptons.

The same applies to the uncertainty of the gamma+jets process. We assign a systematic uncertainty

of 30% inspired by Ref. [36]. The inclusive W/Z cross section is known at NNLO, with an uncertainty of ≈ 5%; we assign conservatively an uncertainty of 20% to the W+jets and Z+jets samples. Similar numbers are found in Ref. [40]. We assign for the W/Z + gamma process a systematic uncertainty of 20%. This is a bit more conservative than the numbers quoted in Ref. [41]. For $t\bar{t}$ and single top, known to NNLO and NLO respectively, an uncertainty of 20% is used [42, 43]. Diboson processes are known to NLO. An uncertainty of 20% is assigned for these processes. Due to the effect of possible jet production we quote a more conservative uncertainty than e.g. Ref. [44]. Finally the large K-factor uncertainty for $W\gamma\gamma$ results in an uncertainty of 100% for this process.

All systematic uncertainties are added in quadrature.

6 Results

6.1 Event yields

The event yields subdivided in channels are presented for the data and Monte Carlo expectations for all channels with at least one data event. Data events are found in 655 analysis channels. Each channel is exclusive, i.e. the list of studied channels includes all combinations with repetition which can be formed out of the electron, muon, photon, b-jet and jets object types. The list also includes classes with a missing transverse momentum object. The data and MC prediction are shown in Figure 1 for the EGamma, in Figure 2 for the Muon and in Figure 3 and 4 for the JetTauEtmiss streams. Only event classes are considered where, within the statistics of the SM Monte Carlo, at least 1 background event is generated. For all channels good agreement between data and SM prediction is observed.

6.2 Search algorithm

In order to quantitatively determine the level of agreement between the data and the SM expectation and to identify regions of possible deviations we use a search algorithm, first developed for the H1 generic search [2]. As a compromise between maximizing the sensitivity and keeping the "look elsewhere" effect [45] at a manageable level, the algorithm is only applied to the effective mass distributions of the events in the 655 channels. The effective mass, m_{eff}, is defined for each event class as the scalar sum of the transverse momenta of the objects defining the channel. This quantity has been widely used in the context of searches for new physics, as it is sensitive to a large class of new physics signals.

The search algorithm locates the region of largest deviation in a distribution of any shape. The bin size of the scanned distributions is chosen to reflect the expected resolution from the objects selected in the given channel. In every histogram the number of data events N_{obs} and the expectation N_{SM} with its total systematic uncertainty δN_{SM} are determined for each possible connected bin region with at least two bins. A statistical estimator p is used to judge which region is of most interest. It is derived from the convolution of a Poisson probability density function (pdf) to account for statistical uncertainties with a Gaussian pdf, $G(b; N_{SM}, \delta N_{SM})$, with mean N_{SM} and width δN_{SM}, to include effects of non negligible systematic uncertainties. It is defined as

$$p = A \int_0^\infty db \, G(b; N_{SM}, \delta N_{SM}) \sum_{i=N_{obs}}^\infty \frac{e^{-b} b^i}{i!} \tag{1}$$

The factor $A = 1/\int_0^\infty db \, G(b; N_{SM}, \delta N_{SM}) \sum_{i=0}^\infty \frac{e^{-b} b^i}{i!}$ ensures that the pdf is normalized to unity. If the Gaussian pdf G is replaced by a Dirac delta function $\delta(b - N_{SM})$ the estimator p results in a usual Poisson probability. The value of p gives an estimate of the probability that the SM expectation fluctuates upwards to the data in a given region. Here p is interpreted as the local p-value of this deviation. The region
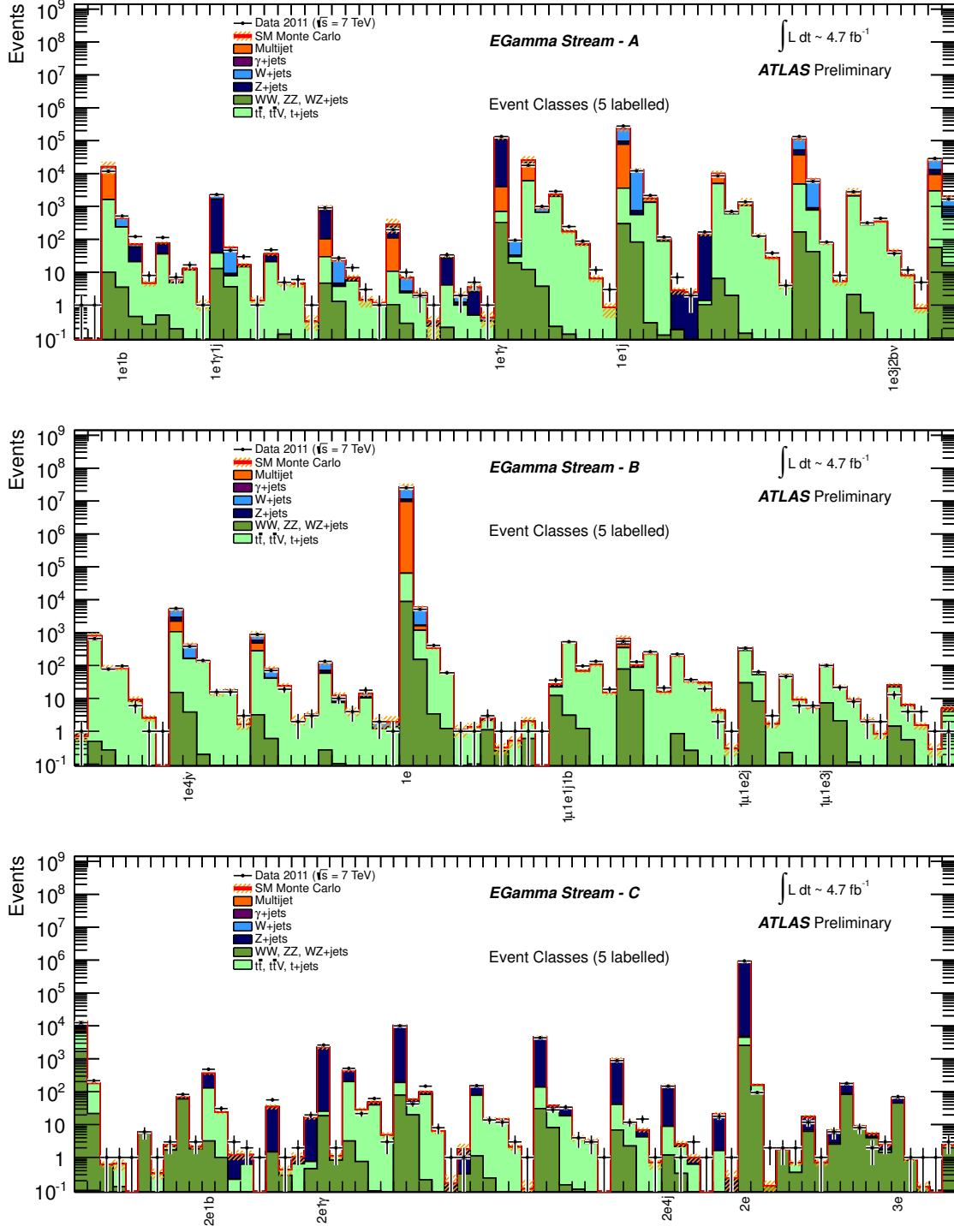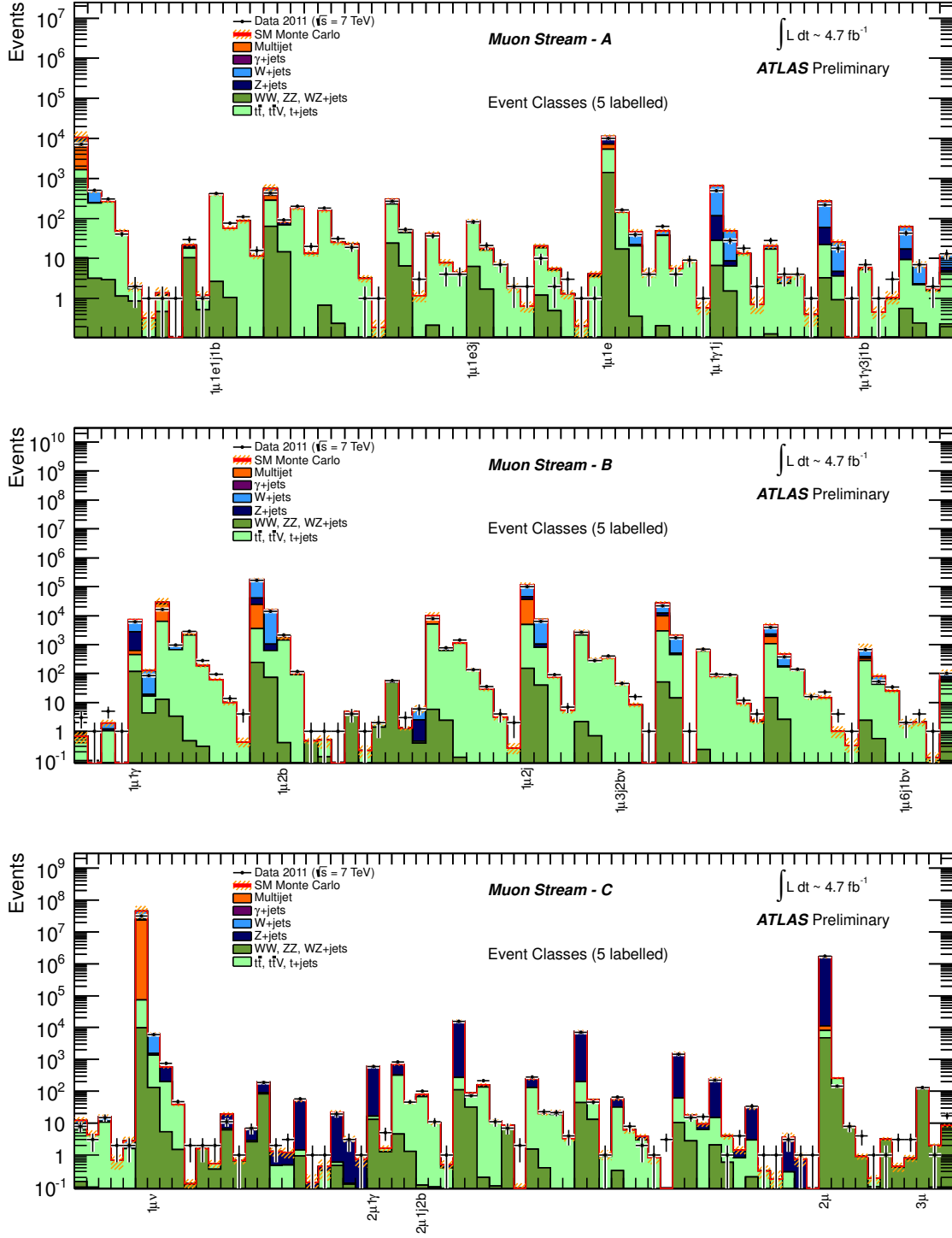
Figure 1: Number of events for event classes in the EGamma stream (parts A, B, C). As an example, 5 classes in each part are labelled according to the frequency and the label type (e, μ, γ, jet j, b-jet b, E_T^{miss} ν) of the reconstructed objects for this event class. The data are compared to several SM background sources as described in the text.
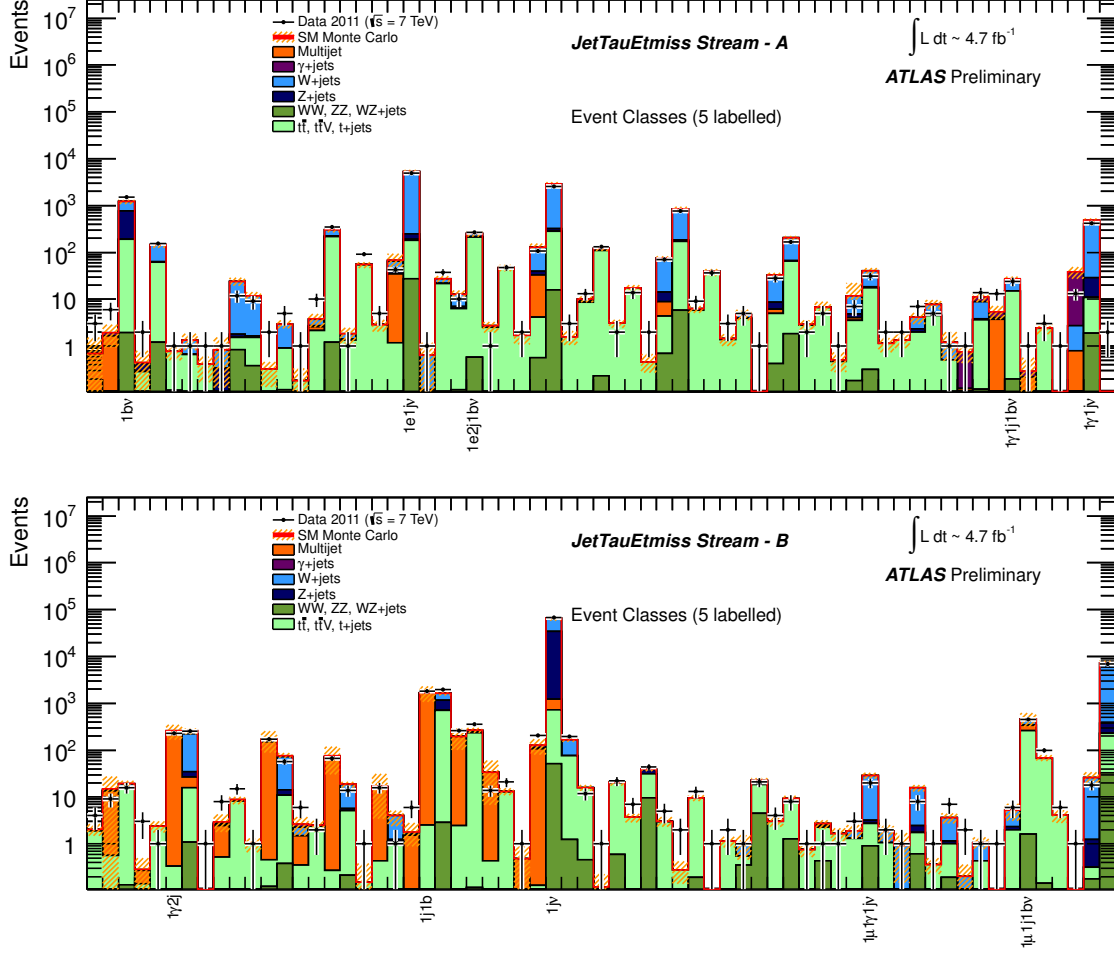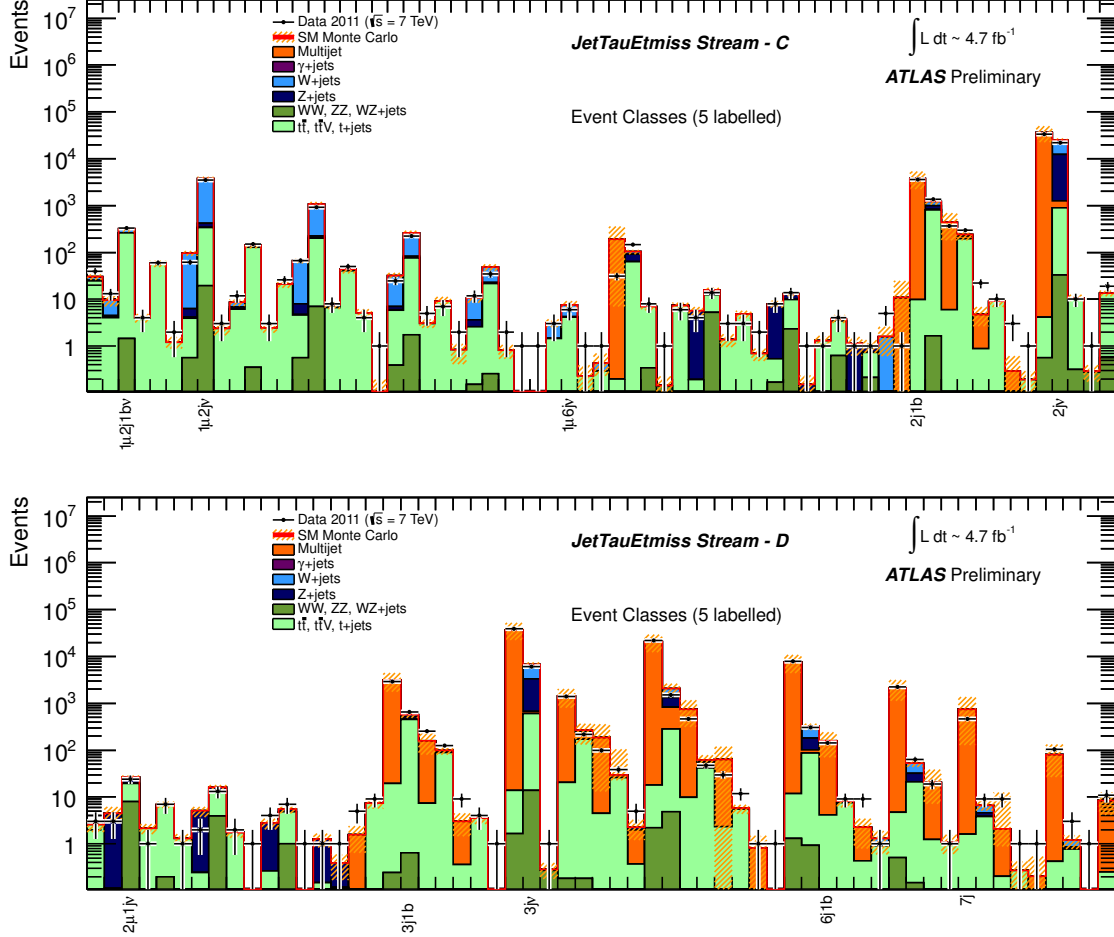
.

7

Figure 2: Number of events for event classes in the Muon Stream (parts A, B, C). As an example, 5 classes in each part are labelled according to the frequency and the label type (e, μ, γ, jet j, b-jet b, E_T^{miss} ν) of the reconstructed objects for this event class. The data are compared to several SM background sources as described in the text.

.

8

Figure 3: Number of events for event classes in the JetTauEtmiss stream (parts A, B). As an example, 5 classes in each part are labelled according to the frequency and the label type (e, μ, γ, jet j, b-jet b, E_T^{miss} ν) of the reconstructed objects for this event class. The data are compared to several SM background sources as described in the text.

9

Figure 4: Number of events for event classes in the JetTauEtmiss stream (parts C, D). As an example, 5 classes in each part are labelled according to the frequency and the label type (e, μ, γ, jet j, b-jet b, E_T^{miss} ν) of the reconstructed objects for this event class. The data are compared to several SM background sources as described in the text.

of greatest deviation found by the algorithm is the region with the smallest p-value. Such a method is able to find narrow resonances and single outstanding events as well as signals spread over large regions of phase space in distributions of any shape. To avoid being sensitive to the effect of poor Monte Carlo statistics, regions where the total background prediction has a relative uncertainty of 100% are discarded by the algorithm.

The probability that somewhere in the event class distribution a statistical fluctuation occurs is modelled by toy experiments. In this procedure, the data are replaced by pseudo data which are generated with the probability density of the Monte Carlo expectation.

6.3 Search Results

Effective mass distributions
Two example distributions of the effective mass are presented for the EGamma stream. Figure 5 shows the event class with one muon, one electron, two jets and $E_\mathrm{T}^\mathrm{miss}$ ($1\mu1e2jv$) and Figure 6 the channel with with two electrons, 3 jets and $E_\mathrm{T}^\mathrm{miss}$ ($2e3jv$). The region of greatest deviation as found by the search algorithm is indicated with vertical lines.

P-value distributions for data and for SM only (toys)
The distribution of the local p-value observed in data, compared to the expectation from the SM hypothesis as obtained from toys, is shown in Figures 7, 8 and 9 for each stream separately. In these figures the statistical uncertainty of the SM toys is shown as a shaded band. No event class is found with a local p-value below 10^{-3}, corresponding roughly to a 3 sigma deviation. This is consistent with the expectation from toy experiments. At least one class with a local p-value below 10^{-3} is expected to be found in about $10 - 20\%$ of the toy experiments per analyzed stream. The analysis has therefore not observed a hint of a signal of new physics. In general, remarkably good agreement between data and Standard Model expectation is found.

It must be stressed that this analysis presents a tool to search for signals of new physics seen as deviations from a pure SM Monte Carlo prediction. If deviations were to be found, they would require more dedicated analyses pursuing a more detailed determination of the Standard Model backgrounds. Also, due to the nature of the general search, this analysis might miss possible deviations from the SM if the MC prediction is too high in a phase space region or if new physics contributions are present on top of a large background.

6.4 Sensitivity to new physics signals

A set of pseudo data samples is generated to test the sensitivity of the analysis procedure to some selected signals of new physics. The prediction of a specific new physics model is added on top of the SM prediction and the sum is used to generate pseudo data samples. A Monte Carlo technique is used to vary the distribution of signal events and to generate many pseudo experiments. The algorithm is run on those pseudo experiments and the distribution of local p-values is derived. A few model supersymmetric points with different sparticle masses on the CMSSM/MSUGRA plane with $\tan\beta = 10$, $A_0 = 0$ and $\mu > 0$ have been tested with different values for the common GUT scale boson and fermion masses (m_0, $m_{1/2}$). The model point (660, 240), with squark masses of 700 GeV and gluino masses of 600 GeV, has a cross section of about 0.8 pb. The point (1220, 180) with gluinos at 500 GeV and squarks at 1200 GeV, has a cross section of 1.12 pb, whereas (1220, 240) has gluinos at 600 GeV and squarks at 1200 GeV with a cross section of 0.2 pb. These supersymmetric models have been excluded already by a previous ATLAS analysis [7].

Figure 10 shows the effect that the additional signal contribution would have on the p-value distribution. A supersymmetric signal would show up in a large number of classes, modifying the shape of the
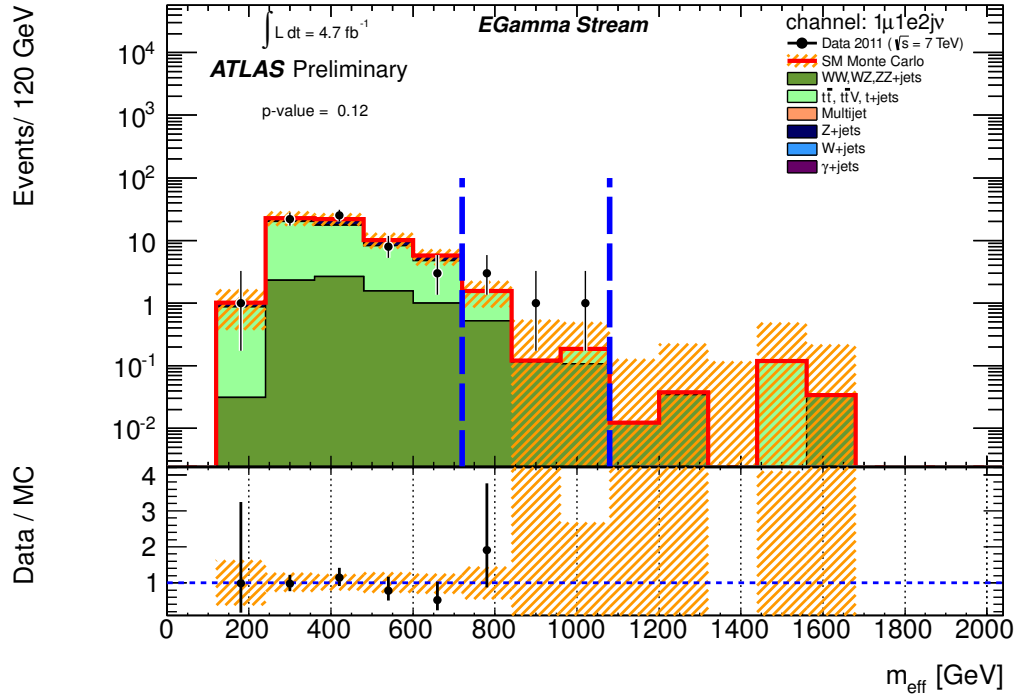
Figure 5: m_{eff} distribution for the event class with one muon, one electron, two jets and $E_{\text{T}}^{\text{miss}}$ ($1\mu 1e 2 j\nu$) in the EGamma stream. The dashed vertical lines indicate the region of interest which has the smallest p-value (0.12) for this event class.
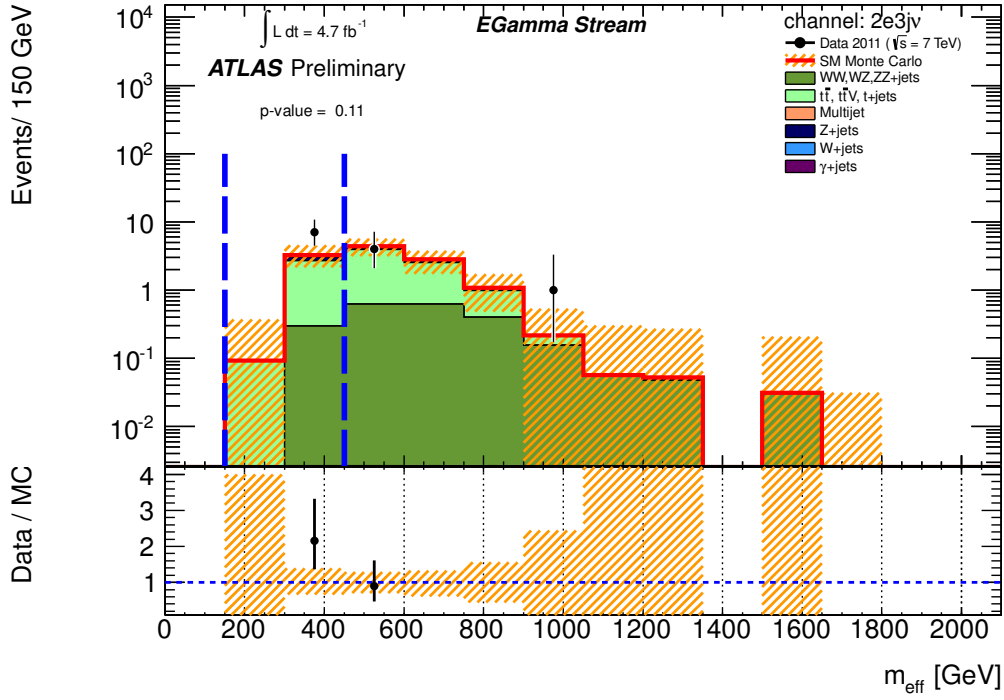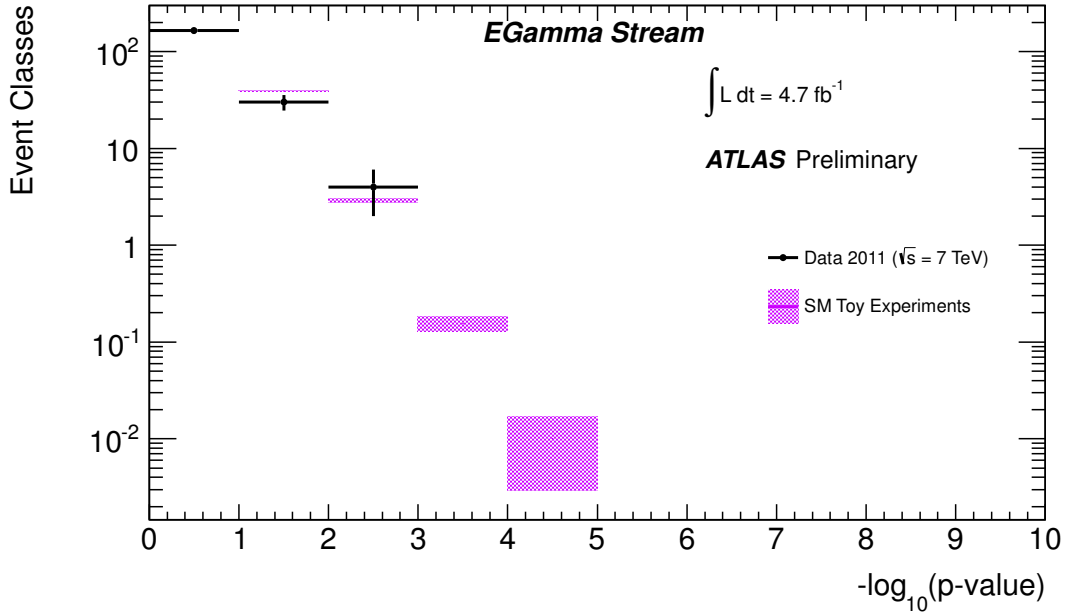
Figure 6: m_{eff} distribution for the event class with two electrons, 3 jets and E_T^{miss} ($2e3j\nu$) in the EGamma stream. The dashed vertical lines indicate the region of interest which has the smallest p-value (0.11) for this event class.

Figure 7: The figure show the observed and expected number of classes in the EGamma stream having a given range in $-\log_{10}(p-\text{value})$. The band for the SM toy experiments represents the uncertainty, due to the statistics of the toy experiments, on the mean expected number of classes.
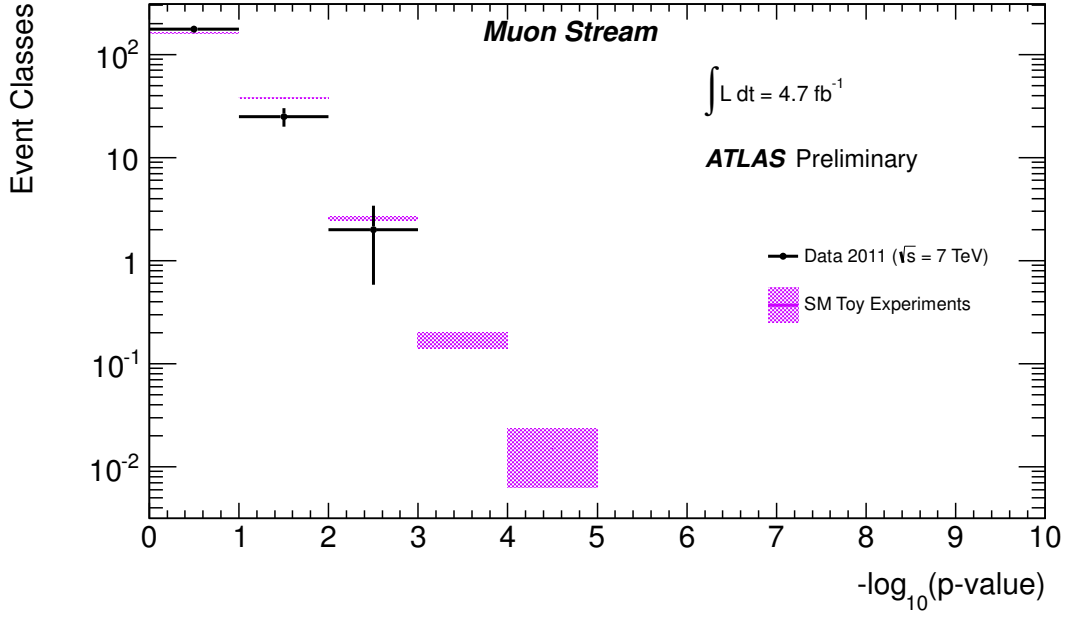
Figure 8: The figure show the observed and expected number of classes in the Muon stream having a given range in $-\log_{10}(p-value)$. The band for the SM toy experiments represents the uncertainty, due to the statistics of the toy experiments, on the mean expected number of classes.
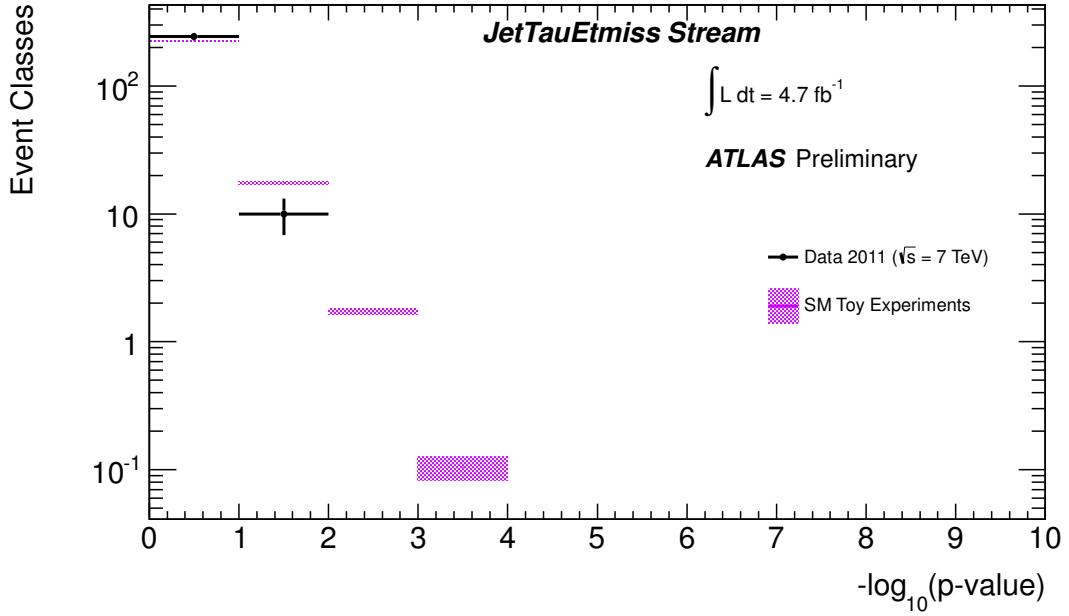

Figure 9: The figure show the observed and expected number of classes in the JetTauEtmiss stream having a given range in $-\log_{10}(p-value)$. The band for the SM toy experiments represents the uncertainty, due to the statistics of the toy experiments, on the mean expected number of classes.

p-value distribution towards higher deviations. The signal point (660, 240), as well as the point (1220, 180) would be clearly visible, mainly in the JetTauEtmiss stream. The signal due to the (1220, 240) model has a smaller impact in the lepton streams, but would still predict in the JetTauEtmiss stream, compared to the SM, a higher number of event classes with large deviations.

7 Conclusion

The data collected with the ATLAS experiment during the year 2011 in pp collisions at $\sqrt{s}$ = 7 TeV, corresponding to an integrated luminosity of 4.7 fb^{-1}, have been used to search for deviations from the SM prediction at high transverse momentum. Event topologies involving isolated electrons, muons, photons, jets, b-jets and missing transverse momentum have been classified systematically. All channels have been scanned for deviations from the SM Monte Carlo prediction in the effective mass distributions. No significant excess above the Monte Carlo prediction has been observed.
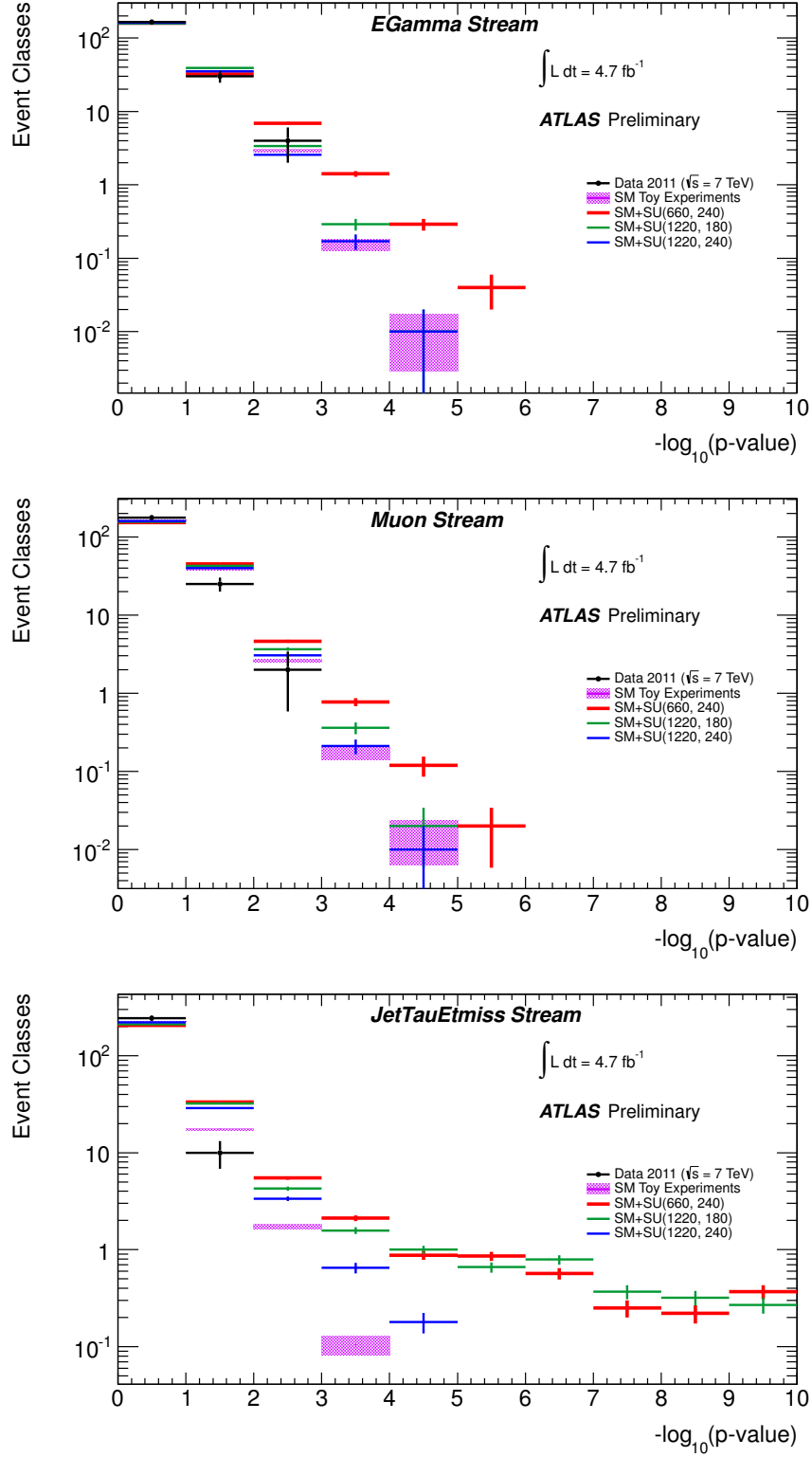
Figure 10: Sensitivity of the search method to supersymmetric signal models, shown for each stream separately. The figure shows the observed and expected number of classes in each stream having a given range in $-\log_{10}(p-value)$. The band for the SM toy experiments represents the uncertainty, due to the statistics of the toy experiments, on the mean expected number of classes. The predicted number of classes are indicated for the three CMSSM/MSUGRA models with $\tan\beta = 10$, $A_0 = 0$ and $\mu > 0$ and the parameter set (m_0, $m_{1/2}$).

16

References

[1] D0 Collaboration, Abbott, B. et al., *Search for new physics in eμX data at DØ using SLEUTH: A quasi-model-independent search strategy for new physics*, Phys. Rev. D **62** (2000) 092004.

[2] H1 Collaboration, A. Aktas et al., *A General search for new phenomena in ep scattering at HERA*, Phys.Lett. **B602** (2004) 14–30, `arXiv:hep-ex/0408044 [hep-ex]`.

[3] CDF Collaboration, Aaltonen, T. et al., *Model-independent and quasi-model-independent search for new physics at CDF*, Phys. Rev. D **78** (2008) 012002, `arXiv:0712.1311 [hep-ex]`.

[4] CMS Collaboration, *Model Unspecific Search for New Physics in pp Collisions at sqrt(s) = 7 TeV*, 2011. CMS-PAS-EXO-10-021.

[5] ATLAS Collaboration, *The ATLAS Experiment at the CERN Large Hadron Collider*, 2008. JINST **3** (2008) S08003.

[6] ATLAS Collaboration, *Luminosity Determination in pp Collisions at $\sqrt{s}$ = 7 TeV using the ATLAS Detector in 2011*, 2011. ATLAS-CONF-2011-116.

[7] ATLAS Collaboration, *Search for squarks and gluinos using final states with jets and missing transverse momentum with the ATLAS detector in $\sqrt{s}$ = 7 TeV proton-proton collisions*, 2012. ATLAS-CONF-2012-033.

[8] T. Sjostrand, S. Mrenna, and P. Z. Skands, *PYTHIA 6.4 Physics and Manual*, JHEP **0605** (2006) 026, `arXiv:hep-ph/0603175`.

[9] A. Sherstnev and R. S. Thorne, *Parton Distributions for LO Generators*, Eur. Phys. J. **C55** (2008) 553–575, `arXiv:0711.2473 [hep-ph]`.

[10] M. L. Mangano et al., *ALPGEN, a generator for hard multiparton processes in hadronic collisions*, JHEP **07** (2003) 001, `arXiv:hep-ph/0206293`.

[11] G. Corcella et al., *HERWIG 6.5: an event generator for Hadron Emission Reactions With Interfering Gluons (including supersymmetric processes)*, JHEP **01** (2001) 010, `arXiv:hep-ph/0011363`.

[12] J. M. Butterworth, J. R. Forshaw, and M. H. Seymour, *Multiparton interactions in photoproduction at HERA*, Z. Phys. **C72** (1996) 637–646, `arXiv:hep-ph/9601371`.

[13] D. Stump et al., *Inclusive jet production, parton distributions, and the search for new physics*, JHEP **0310** (2003) 046, `arXiv:hep-ph/0303013 [hep-ph]`.

[14] Anastasiou, C. et al., *High precision QCD at hadron colliders: Electroweak gauge boson rapidity distributions at NNLO*, Phys.Rev. **D69** (2004) 094008, `arXiv:hep-ph/0312266 [hep-ph]`.

[15] ATLAS Collaboration, *Measurement of the cross-section for b-jets produced in association with a Z boson at sqrt(s)=7 TeV with the ATLAS detector*, Phys.Lett. **B706** (2012) 295–313, `arXiv:1109.1403 [hep-ex]`.

[16] ATLAS Collaboration, *Measurement of the cross section for the production of a W boson in association with b-jets in pp collisions at sqrt(s) = 7 TeV with the ATLAS detector*, Phys.Lett. **B707** (2012) 418–437, `arXiv:1109.1470 [hep-ex]`.

[17] J. Alwall et al., *MadGraph 5 : Going Beyond*, JHEP **1106** (2011) 128, `arXiv:1106.0522 [hep-ph]`.

[18] G. Bozzi, F. Campanario, M. Rauch, and D. Zeppenfeld, *Zγγ production with leptonic decays and triple photon production at NLO QCD*, Phys.Rev. **D84** (2011) 074028, `arXiv:1107.3149 [hep-ph]`.

[19] G. Bozzi, F. Campanario, M. Rauch, and D. Zeppenfeld, *$W^{+-}γγ$ production with leptonic decays at NLO QCD*, Phys.Rev. **D83** (2011) 114035, `arXiv:1103.4613 [hep-ph]`.

[20] S. Frixione and B. R. Webber, *Matching NLO QCD computations and parton shower simulations*, JHEP **06** (2002) 029, `arXiv:hep-ph/0204244`.

[21] S. Frixione and B. R. Webber, *The MC@NLO 3.2 event generator*, `arXiv:hep-ph/0601192 [hep-ph]`.

[22] S. Moch and P. Uwer, *Heavy-quark pair production at two loops in QCD*, Nucl.Phys.Proc.Suppl. **183** (2008) 75–80, `arXiv:0807.2794 [hep-ph]`.

[23] H.-L. Lai et al., *New parton distributions for collider physics*, Phys.Rev. **D82** (2010) 074024, `arXiv:1007.2241 [hep-ph]`.

[24] A. Kardos, Z. Trocsanyi, and C. Papadopoulos, *Top quark pair production in association with a Z-boson at NLO accuracy*, Phys.Rev. **D85** (2012) 054015, `arXiv:1111.0610 [hep-ph]`.

[25] J. M. Campbell and R. K. Ellis, *$t\bar{t}W$ production and decay at NLO*, JHEP **1207** (2012) 052, `arXiv:1204.5678 [hep-ph]`.

[26] W. Kilian, T. Ohl, and J. Reuter, *WHIZARD: Simulating Multi-Particle Processes at LHC and ILC*, Eur.Phys.J. **C71** (2011) 1742, `arXiv:0708.4233 [hep-ph]`.

[27] M. Bahr et al., *Herwig++ Physics and Manual*, Eur. Phys. J. **C58** (2008) 639–707, `arXiv:0803.0883 [hep-ph]`.

[28] W. Beenakker, R. Hopker, M. Spira, and P. M. Zerwas, *Squark and gluino production at hadron colliders*, Nucl. Phys. **B492** (1997) 51–103, `arXiv:hep-ph/9610490`.

[29] ATLAS Collaboration, *Charged particle multiplicities in p p interactions at $\sqrt{s}$ = 0.9 and 7 TeV in a diffractive limited phase-space measured with the ATLAS detector at the LHC and new PYTHIA6 tune*, 2010. ATLAS-CONF-2010-031.

[30] ATLAS Collaboration, *The ATLAS Simulation Infrastructure*, Eur. Phys. J. **C70** (2010) 823–874, `arXiv:1005.4568 [physics.ins-det]`.

[31] M. Cacciari, G. P. Salam, and G. Soyez, *The anti-k_t jet clustering algorithm*, JHEP **04** (2008) 063, `arXiv:0802.1189 [hep-ph]`.

[32] M. Cacciari and G. P. Salam, *Dispelling the N^3 myth for the k_t jet-finder*, Phys. Lett. **B641** (2006) 57–61, `arXiv:hep-ph/0512210`.

[33] ATLAS Collaboration, *Jet energy scale and its systematic uncertainty in proton-proton collisions at $\sqrt{s}$ = 7 TeV in ATLAS 2010 data*, 2010. ATLAS-CONF-2011-032.

[34] ATLAS Collaboration, *Commissioning of the ATLAS high-performance b-tagging algorithms in the 7 TeV collision data*, 2011. ATLAS-CONF-2011-102.

[35] ATLAS Collaboration, *Measurement of the W → ℓν and Z/γ* → ℓℓ production cross sections in proton-proton collisions at* $\sqrt{s}$ *= 7 TeV with the ATLAS detector*, JHEP **1012** (2010) 060, arXiv:1010.2130 [hep-ex].

[36] ATLAS Collaboration, *Measurement of the production cross section of an isolated photon associated with jets in proton-proton collisions at sqrt(s) = 7 TeV with the ATLAS detector*, Phys.Rev. **D85** (2012) 092014, arXiv:1203.3161 [hep-ex].

[37] ATLAS Collaboration, *Expected Performance of the ATLAS Experiment - Detector, Trigger and Physics*, CERN-OPEN-2008-020. arXiv:0901.0512 [hep-ex].

[38] ATLAS Collaboration, *Search for supersymmetry using final states with one lepton, jets, and missing transverse momentum with the ATLAS detector in* $\sqrt{s}$ *= 7 TeV pp collisions*, Phys. Rev. Lett. **106** (2011) , arXiv:1102.2375 [hep-ph].

[39] ATLAS Collaboration, *Measurement of multi-jet cross sections in proton-proton collisions at a 7 TeV center-of-mass energy*, Eur.Phys.J. **C71** (2011) 1763, arXiv:1107.2092 [hep-ex].

[40] ATLAS Collaboration, *Measurement of the production cross section for Z/gamma* in association with jets in pp collisions at sqrt(s) = 7 TeV with the ATLAS detector*, Phys.Rev. **D85** (2012) 032009, arXiv:1111.2690 [hep-ex].

[41] ATLAS Collaboration, *Measurement of W gamma and Z gamma production cross sections in pp collisions at sqrt(s) = 7 TeV and limits on anomalous triple gauge couplings with the ATLAS detector*, arXiv:1205.2531 [hep-ex].

[42] ATLAS Collaboration, *Measurement of the top quark pair production cross-section with ATLAS in the single lepton channel*, Phys.Lett. **B711** (2012) 244–263, arXiv:1201.1889 [hep-ex].

[43] ATLAS Collaboration, *Measurement of the t-channel single top-quark production cross section in pp collisions at sqrt(s) = 7 TeV with the ATLAS detector*, arXiv:1205.3130 [hep-ex].

[44] ATLAS Collaboration, *Measurement of the WW cross section in sqrt(s) = 7 TeV pp collisions with the ATLAS detector and limits on anomalous gauge couplings*, Phys.Lett. **B712** (2012) 289–308, arXiv:1203.6232 [hep-ex].

[45] E. Gross and O. Vitells, *Trial factors for the look elsewhere effect in high energy physics*, Eur. Phys. J. **C70** (2010) 525, arXiv:1005.1891 [physics.data-an].